

ANGULAR DISTRIBUTIONS OF TARGET
FRAGMENTS IN ^{84}Kr -Em AND ^{16}O -Em
COLLISIONS AT HIGH ENERGIES

FU-HU LIU[†], N.N. ABD ALLAH^{a,b}, B.K. SINGH^{a,c}, T. AHMAD^{a,d}

^aPhysics Department, Shanxi University, Taiyuan, Shanxi 030006, China

^bPhysics Department, Faculty of Science, South Valley University, Sohag, Egypt

^cPhysics Department, Banaras Hindu University, Varanasi 221005, India

^dUniversity Polytechnic, Aligarh Muslim University, Aligarh 202002, India

(Received January 3, 2006; revised version received April 13, 2006)

A multisource ideal gas model is used to give an uniform description of the angular distributions of different kinds of target fragments produced in nucleus–nucleus collisions at high energies. The theoretical results calculated by the Monte Carlo method are qualitatively in agreement with the experimental angular distributions of target black, grey, and heavy fragments produced in ^{84}Kr -Emulsion (Em) collisions at 1.7 AGeV and ^{16}O -Em collisions at 3.7 and 60 AGeV.

PACS numbers: 25.70.Mn, 25.70.Pq

1. Introduction

Target fragmentation is an important experimental phenomenon in nucleus–nucleus collisions at intermediate and high energies [1–3]. It can provide information about the nuclear reaction mechanism [4–6] and is highly important for us. A few AGeV is a special energy, at which the nuclear limiting fragmentation [7–9] applies initially. To study nuclear reaction at a few AGeV and above energy is of great importance.

Recently, angular distributions of target fragments produced in silicon-emulsion collisions at 4.5 AGeV/ c [10] and magnesium-emulsion collisions at 4.5 AGeV/ c [11] were studied by us, and a multisource ideal gas model was introduced. It was shown that the model gave acceptable descriptions of the angular distributions of target fragments in nucleus-emulsion collisions at 4.5 AGeV/ c .

[†] e-mail: fuhuliu@163.com

The aim of the present work is to perform an investigation of angular distributions of target fragments produced in krypton-emulsion collisions at 1.7 AGeV and oxygen-emulsion collisions at 3.7 and 60 AGeV. Comparing with our previous work [10,11], we notice that the concerned energy range is extended to 1.7–60 AGeV and the incident nucleus is extended to ^{84}Kr and ^{16}O . We hope to see the characteristics of angular distributions of target fragments in ^{84}Kr -Em and ^{16}O -Em collisions at high energies and to test the multisource ideal gas model in the present work.

2. The model

The model used in the present work is called the multisource ideal gas model which can be found in our previous work [10,11]. To give a whole presentation of the present work, we introduce the model shortly in the following. Let the beam direction be the oz axis and the reaction plane be the yo z plane. Many emission sources of particles are assumed to be formed in high-energy nucleus–nucleus collisions. In the rest frame of the emission source i , as in the Maxwell's ideal gas model, we assume that the particles are emitted isotropically and the three components p'_x , p'_y , and p'_z of particle momentum obey a Gaussian distribution having the same standard deviation σ_i .

Considering the movement of the emission source and the interactions between emission sources, the particle momentum components p_x , p_y , and p_z in the final state in the laboratory reference frame are different from those in the rest frame of the emission source. The simplest relations between p_x and p'_x , p_y and p'_y , and p_z and p'_z are linear

$$p_x = a_x p'_x + B_x = a_x p'_x + b_x \sigma_i, \quad (1)$$

$$p_y = a_y p'_y + B_y = a_y p'_y + b_y \sigma_i, \quad (2)$$

and

$$p_z = a_z p'_z + B_z = a_z p'_z + b_z \sigma_i, \quad (3)$$

where B_x , B_y , and B_z are free parameters that can be rewritten as $b_x \sigma_i$, $b_y \sigma_i$, and $b_z \sigma_i$, respectively. σ_i is the parameter that characterizes the width of the momentum distribution in the source reference frame. a_x , b_x , a_y , b_y , a_z , and b_z are free parameters.

It seems that the above formalism is in contraction with Lorentz transformation. We would like to point out that one could understand the current formalism because Eqs. (1)–(3) represented the relations of “mean” momenta between the cases of laboratory reference frame and source rest frame. Let R_1 , R_2 , R_3 , R_4 , R_5 , and R_6 denote random variables distributed in $[0,1]$, we have

$$p'_x = \sqrt{-2 \ln R_1} \cos(2\pi R_2) \sigma_i, \quad (4)$$

$$p'_y = \sqrt{-2 \ln R_3} \cos(2\pi R_4) \sigma_i, \tag{5}$$

and

$$p'_z = \sqrt{-2 \ln R_5} \cos(2\pi R_6) \sigma_i, \tag{6}$$

because p'_x , p'_y , and p'_z obey a Gaussian distribution law.

The emission angle θ of a target fragment in the laboratory reference frame is given by

$$\theta = \arctan \frac{\sqrt{p_x^2 + p_y^2}}{p_z}. \tag{7}$$

Considering Eqs. (1)–(6), we have

$$\theta = \arctan \frac{\sqrt{[a_x \sqrt{-2 \ln R_1} \cos(2\pi R_2) + b_x]^2 + [a_y \sqrt{-2 \ln R_3} \cos(2\pi R_4) + b_y]^2}}{a_z \sqrt{-2 \ln R_5} \cos(2\pi R_6) + b_z}. \tag{8}$$

The theoretical results can be given by the Monte Carlo method and statistics. For an isotropic emission source, *i.e.* in the case of $a_x(a_y, a_z) = 1$ and $b_x(b_y, b_z) = 0$, we have the angular distribution to be

$$f(\theta) = \frac{1}{2} \sin \theta. \tag{9}$$

There are relations between the parameter values and the shapes of emission sources. In the momentum space, the emission source shapes in x , y , and z directions can be described by a_x and b_x , a_y and b_y , as well as a_z and b_z , respectively. $a_x > 1$, $a_x = 1$, and $a_x < 1$ mean an extension, a constancy (a Gaussian distribution), and a compression of the emission source in the x direction, respectively. The meanings of a_y and a_z are similar to that of a_x . Because we concern only the relative values of a_x , a_y , and a_z , the values of a_x , a_y , and a_z can be limited to be greater than or equal to 1. Then, $a_x(a_y, a_z) > 1$ and $a_x(a_y, a_z) = 1$ mean an extension and a constancy of the emission source in the $x(y, z)$ direction, respectively. The parameter $b_x > 0$, $= 0$, and < 0 mean that the center of emission source has a movement along the positive x direction, is in a static state, and has a movement along the negative x direction, respectively. The meanings of b_y and b_z are similar to that of b_x .

3. Comparison with experimental results

Fig. 1 presents the angular distributions of target fragments produced in ^{84}Kr -Em collisions at 1.7 AGeV. Figs. 1(a), 1(b), and 1(c) correspond to the results of black, grey, and heavy fragments, respectively. The histograms are the experimental results of Ref. [12], and the curves are our calculated results which will be discussed later on. Fig. 2 is similar to Fig. 1, but it is for ^{16}O -Em collisions at 3.7 AGeV. The experimental results are taken from Ref. [13]. Figure 3 is similar to Fig. 1, too, but it is for ^{16}O -Em collisions at 60 AGeV. The experimental results are taken from Ref. [14]. From Figs. 1, 2 and 3 one can see that the results corresponding to black, grey, and heavy fragments are similar, respectively for three different kinds of collisions. But the results corresponding to black, grey, and heavy fragments are different from each other.

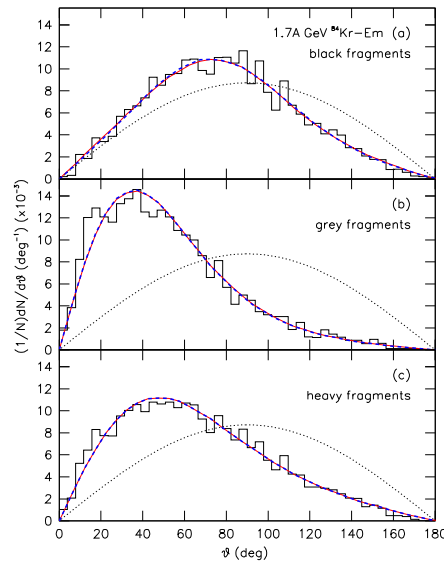


Fig. 1. Angular distributions of target black (a), grey (b), and heavy (c) fragments produced in ^{84}Kr -Em collisions at 1.7 AGeV. The histograms are the experimental results of Ref. [12]. The curves are our calculated results.

To investigate the dependence of angular distributions of target fragments on the multiplicity of target fragments (Nh), Figs. 4 and 5 show the angular distributions of target fragments produced in 60 AGeV ^{16}O -Em collisions with $Nh < 8$ and $Nh \geq 8$, respectively. The histograms are the experimental results of Ref. [14], and the curves are our calculated results. We notice that there is no obvious difference between the two subsamples.

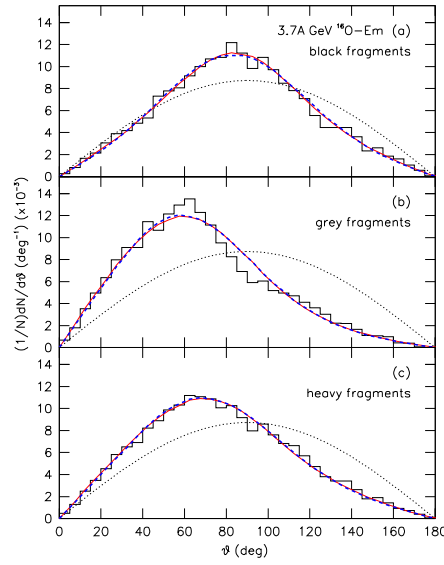


Fig. 2. Angular distributions of target black (a), grey (b), and heavy (c) fragments produced in ^{16}O -Em collisions at 3.7 AGeV. The histograms are the experimental results of Ref. [13]. The curves are our calculated results.

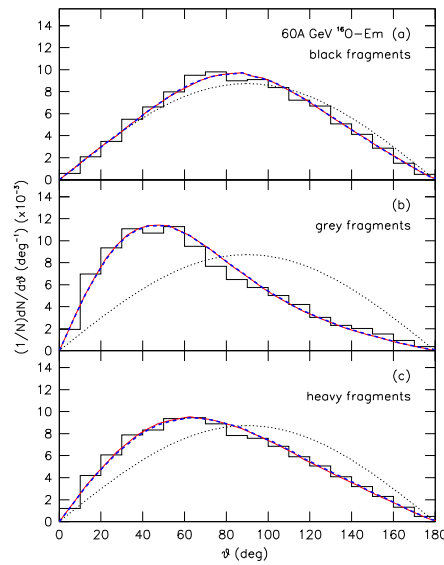


Fig. 3. Angular distributions of target black (a), grey (b), and heavy (c) fragments produced in ^{16}O -Em collisions at 60 AGeV. The histograms are the experimental results of Ref. [14]. The curves are our calculated results.

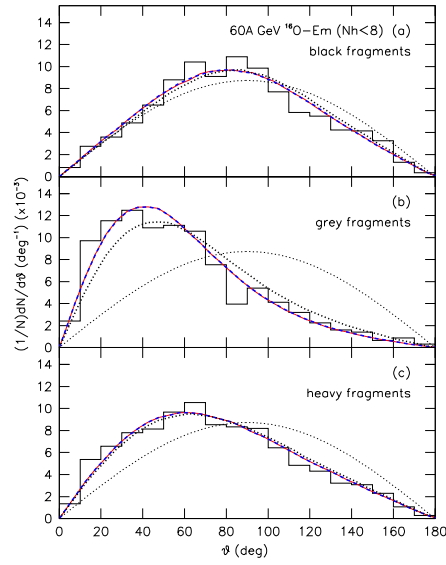


Fig. 4. Angular distributions of target black (a), grey (b), and heavy (c) fragments produced in $^{16}\text{O-Em}$ collisions with $Nh < 8$ at 60 AGeV. The histograms are the experimental results of Ref. [14]. The curves are our calculated results.

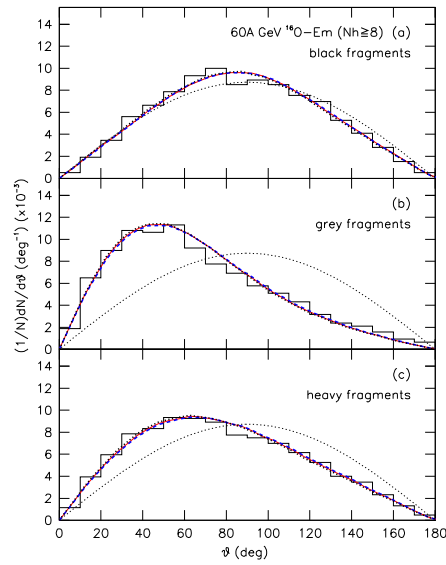


Fig. 5. Angular distributions of target black (a), grey (b), and heavy (c) fragments produced in $^{16}\text{O-Em}$ collisions with $Nh \geq 8$ at 60 AGeV. The histograms are the experimental results of Ref. [14]. The curves are our calculated results.

In Figs. 4 and 5, a comparison of distributions is made for subsamples of events with $Nh < 8$ and $Nh \geq 8$. The emulsion is a composite target. The interactions in emulsion can be separated into samples of events with hydrogen, light (C,N,O) and heavy (Ag,Br) target nuclei. According to Ref. [15], this separation is accomplished using two slightly different methods. One is based on the correlation between the number, N_π , of charged particles produced and the number Nb of black fragments from target nuclei; the other on the number Nh of target fragments and the cut imposed on N_π . We would like to point out that the meaning of target fragments used here is the black fragments plus recoil protons. In Figs. 4 and 5, the experimental data do not show the dependence of angular distributions of target fragments on the target size, but the multiplicity of target fragments. If we regard approximately the events with $Nh < 8$ and $Nh \geq 8$ as interactions on "HCNO" and "AgBr", respectively, this incomplete separation procedure is only acceptable for testing the model considered.

In Figs. 1–5, our calculated results are given by curves. The thin dotted curves in the figures are the result of an isotropic emission. The experimental data do not show an isotropic emission. The solid curves are our calculated results by a set of parameter values given in the left panel of Table I. The dashed curves are our calculated results by another set of parameter values given in the right panel of Table I. The two sets of parameter values are obtained by fitting the experimental data and the χ^2 -testing is used in

TABLE I

Parameter values for solid (left panel) and dashed (right panel) curves in Figs. 1–5. The values of $a_{x,y,z}$ and $b_{x,y,z}$ for a static source are 1 and 0, respectively.

Figs.	a_x	a_y	a_z	b_x	b_y	b_z	a_x	a_y	a_z	b_x	b_y	b_z
1(a)	1.20	1.20	1	0	0	0.35	1	1	1	0.65	0.65	0.35
1(b)	1.05	1.05	1.05	0	0	1.20	1	1	1	0	0	1.15
1(c)	1.05	1.05	1.05	0	0	0.72	1	1	1	0	0	0.68
2(a)	1.28	1.28	1	0	0	0.15	1	1	1	0.75	0.75	0.15
2(b)	1.20	1.20	1	0	0	0.70	1	1	1	0.65	0.65	0.70
2(c)	1.18	1.18	1	0	0	0.43	1	1	1	0.62	0.62	0.43
3(a)	1.10	1.10	1	0	0	0.10	1	1	1	0.45	0.45	0.10
3(b)	1.05	1.05	1.05	0	0	0.80	1	1	1	0	0	0.72
3(c)	1.05	1.05	1.05	0	0	0.36	1	1	1	0	0	0.33
4(a)	1.10	1.10	1	0	0	0.15	1	1	1	0.45	0.45	0.15
4(b)	1.05	1.05	1.05	0	0	0.98	1	1	1	0	0	0.93
4(c)	1.05	1.05	1.05	0	0	0.40	1	1	1	0	0	0.38
5(a)	1.10	1.10	1	0	0	0.08	1	1	1	0.45	0.45	0.08
5(b)	1.05	1.05	1.05	0	0	0.75	1	1	1	0	0	0.70
5(c)	1.05	1.05	1.05	0	0	0.34	1	1	1	0	0	0.31

the calculation. We see that different sets of parameter values give almost the same results. The parameter values in the left panel of Table I render that the emission sources have extensions and movements in the momentum space, while the parameter values in the right panel of Table I render that the emission sources have only movements. From space angular distribution, we cannot test which one of the two sets of parameter values is better. Azimuthal distribution is needed to give a combined testing in future.

For a comparison, the solid curves in Figs. 3(a), 3(b), and 3(c) are shown in Figs. 4(a), 4(b), and 4(c), as well as in Figs. 5(a), 5(b), and 5(c), by the thick dotted curves, respectively. An obvious difference is observed between the solid (dashed) curves and the thick dotted curves in angular distribution of grey fragments produced in ^{16}O -Em collisions with $Nh < 8$ at 60 AGeV. There is no obvious difference between the solid (dashed) curves and the thick dotted curves in angular distribution of grey fragments produced in ^{16}O -Em collisions with $Nh \geq 8$ at the same incident energy. For black and heavy fragments, there is no obvious difference between the two types of curves for the two kinds of collisions. This means that the grey fragments in ^{16}O -Em collisions with $Nh < 8$ has less contribution for the final state target fragments.

4. Discussions and conclusions

The space angular distributions of black, grey, and heavy fragments produced in krypton-emulsion collisions at 1.7 AGeV and oxygen-emulsion collisions at 3.7 and 60 AGeV have been analyzed uniformly by the multisource ideal gas model. An obvious difference between the angular distributions of black and grey fragments are observed. This renders that the black and grey fragments have different emission mechanisms. The black fragments are evaporated from the target spectator, and the grey fragments are produced in the target participant and spectator by the cascade collision processes, where the target participant and spectator are concepts in the participant-spectator model [16]. For black, grey, or heavy fragments, the angular distribution does not depend obviously on the projectile size and incident energy. Target limiting fragmentation is observed in the concerned energy range.

The angular distribution of target black fragments does not show an obvious difference for light and heavy target at 60 AGeV. This renders that the target black fragments do not remember their emission sources. For the angular distribution, the production of target black fragments does not depend on the multiplicity of target fragments, and the connection between the spectator and participant is very weak. The production of target grey fragments depends on the multiplicity of target fragments. Heavy target contributes to more fragments with large angles.

We have chosen the multisource ideal gas model to analyze the experimental data due to that the target black fragments are nucleons or light nuclei evaporated from the excited target spectator. Maybe, a liquid-gas phase transition happened in the excited target spectator. We have assumed the excited target spectator to be an ideal gas of nucleons and light nuclei. Target grey fragments are mostly recoil protons from the target participant and spectator. Except for the target spectator, the target participant are assumed to be an ideal gas of nucleons. Different kinds of target fragments have different production mechanisms. The present work shows that the multisource ideal gas model (Eq. (8)) describes uniformly the angular distributions of target black, grey, and heavy fragments.

Although a lot of models have been introduced to describe the particle production in nucleus–nucleus collisions at high energies, most of them do not concern the production of target fragments. The multisource ideal gas model is successful in the description of angular distributions of target fragments produced in nucleus–nucleus collisions at high energies [10, 11]. Our previous work shown that the distributions of multiplicity, transverse energy [17], transverse momentum [18], and flow [19] of produced particles, as well as the target fragment flow [20] can be also described by the model.

Comparison with a ball, an extension of the emission source in both the transverse and longitudinal directions in momentum space has been observed. The parameter values describe the shape of the emission source. If we assume that the emission source is a ball in momentum space in the laboratory reference frame, then $a_x > 1$ and $a_x = 1$ mean an extension and a constancy (a Gaussian distribution) of the emission source in the x direction, respectively, and $b_x > 0$, $b_x = 0$, and $b_x < 0$ mean that the center of the emission source has a movement along the positive x direction, is in a static state, and has a movement along the negative x direction, respectively. The meanings of a_y and a_z are similar to that of a_x , and the meanings of b_y and b_z are similar to that of b_x .

This work was supported by the National Natural Science Foundation of China (NSFC) Grants Nos. 10275042 and 10475054, the Shanxi Provincial Foundation for Returned Overseas Scholars Grant No. JLGB(2001)15, the Shanxi Provincial Foundation for Natural Sciences Grant No. 20021006, and the Shanxi Provincial Foundation for Key Subjects Grant No. JJJC(2002)4.

REFERENCES

- [1] D. Ghosh, A. Deb, S.I. Ahmed, P. Ghosh, *Rom. J. Phys.* **48**, 875 (2003).
- [2] V. Singh, S.K. Tuli, B. Bhattacharjee, S. Sengupta, A. Mukhopadhyay, [nucl-ex/0412049](#).
- [3] F.H. Liu, *Chin. J. Phys.* **40**, 159 (2002).
- [4] D. Ghosh, A. Deb, M. Mondal, K.K. Patra, J. Ghosh, *J. Phys. G* **31**, 1083 (2005).
- [5] D. Ghosh, A. Deb, S. Bhattacharyya, J. Ghosh, *Int. J. Mod. Phys.* **E13**, 737 (2004).
- [6] M. El-Nadi, N. Ali-Mossa, A. Abdelsalam, *Nuovo Cimento* **A110**, 1255 (1997).
- [7] B.H. Sa, Z.D. Su, A. Tai, D.M. Zhou, [nucl-th/0309070](#).
- [8] R. Nouicer *et al.* (PHOBOS Collaboration), Proceedings of 37th Rencontres de Moriond on QCD and Hadronic Interactions, Les Arcs, France, 16–23 March, 2002, [nucl-ex/0208003](#).
- [9] A. Jipa *et al.*, *Rom. Rep. Phys.* **56**, 577 (2004).
- [10] F.H. Liu, N.N. Abd Allah, D.H. Zhang, M.Y. Duan, *Int. J. Mod. Phys.* **E12**, 713 (2003).
- [11] F.H. Liu, N.N. Abd Allah, D.H. Zhang, M.Y. Duan, *Chin. J. Phys.* **42**, 152 (2004).
- [12] X.Q. Li, Master Degree Thesis, Shanxi Normal University, Linfen, Shanxi, China, 2005.
- [13] F.J. Wu, Master Degree Thesis, Shanxi Normal University, Linfen, Shanxi, China, 2004.
- [14] F. Liu, Master Degree Thesis, Shanxi Normal University, Linfen, Shanxi, China, 2005.
- [15] M.L. Cherry *et al.*, *Euro. Phys. J.* **C5**, 641 (1998).
- [16] R.J. Glauber, in *Lectures of Theoretical Physics*, Vol. 1, eds W.E. Brittin and L.G. Dunham, Interscience, New York 1959, p. 315.
- [17] F.H. Liu, D.H. Zhang, M.Y. Duan, N.N. Abd Allah, *Chin. J. Phys.* **41**, 618 (2003).
- [18] F.H. Liu, *Chin. J. Phys.* **41**, 357 (2003).
- [19] F.H. Liu, *Europhys. Lett.* **63**, 193 (2003).
- [20] F.H. Liu, N.N. Abd Allah, B.K. Singh, *Phys. Rev.* **C69**, 057601 (2004).